Available online at www.sciencedirect.com

ScienceDirect

www.elsevier.com/locate/jes

JES JOURNAL OF ENVIRONMENTAL SCIENCES

www.jesc.ac.cn

Research Article

Degradation of iopamidol in the permanganate/sulfite process: Evolution of iodine species and effect on the subsequent formation of disinfection by-products

Yimin Lin[1], *Hongyu Dong*[2], *Yating Zhu*[1], *Gongming Zhou*[1], *Junlian Qiao*[1,*], *Xiaohong Guan*[1]

[1] *State Key Laboratory of Pollution Control and Resources Reuse, College of Environmental Science and Engineering, Tongji University, Shanghai 200092, China*

[2] *Department of Environmental Science, School of Ecological and Environmental Sciences, East China Normal University, Shanghai 200241, China*

ARTICLE INFO

Article history:
Received 5 October 2022
Revised 24 November 2022
Accepted 27 November 2022
Available online 6 December 2022

Keywords:
Permanganate/sulfite
Iopamidol
Sulfate radical
Iodinated disinfection byproducts
Pre-oxidation

ABSTRACT

Permanganate/sulfite (Mn(VII)/S(IV)) process is a promising pre-oxidation technology for sequestering the emerging organic contaminants in drinking water treatment plant. Iopamidol (IPM), a representative of iodinated X-ray contrast media, has been widely detected in water sources and has the risk of forming iodinated disinfection byproducts (I-DBPs) in water treatment system. In this study, we investigated the evolution of iodine species during the IPM degradation by the Mn(VII)/S(IV) process and its effect on the subsequent formation of I-DBPs during chlorination at pH 7.0 and 8.0. IPM could be effectively degraded in the Mn(VII)/S(IV) process at environmentally relevant pH (pH 7.0 and 8.0). The results of quenching and competitive oxidation kinetic experiments revealed that $SO_4^{\cdot-}$ was the major reactive oxidizing species contributing to the degradation of IPM whereas the contributions of $HO^{\cdot}$ and reactive manganese species were negligible in the Mn(VII)/S(IV) process. I^- and IO_3^- were generated while no HOI was detected during the degradation of IPM in the Mn(VII)/S(IV) process. The effects of IPM oxidation by Mn(VII)/S(IV) on the subsequent formation of chlorinated disinfection by-products (Cl-DBPs) during chlorination were related to the category of Cl-DBPs. The pre-oxidation of IPM by Mn(VII)/S(IV) resulted in the generation of I-DBPs during the disinfection process although no I-DBPs were detected if no pre-oxidation was applied. The finding of this study suggested that attention should be paid to the toxicity of DBPs when water containing iodinated organic contaminants is treated by Mn(VII)/S(IV) process or other pre-oxidation technologies.

* Corresponding author.
E-mail: qiaoqiao@tongji.edu.cn (J. Qiao).

https://doi.org/10.1016/j.jes.2022.11.020
1001-0742/

Introduction

Disinfection is the important part in the water treatment system to guarantee water supply safety. Due to their power of killing microorganisms, chemical oxidants (e.g., chlorine, chlorine dioxide, ozone, and chloramines) were introduced as disinfectants in municipal water treatment since the early 20th century (McGuire, 2006). However, these disinfectants can react with water matrix to generate disinfection by-products (DBPs) (Richardson et al., 2007), which pose the risk for public health. To date, more than 800 DBPs have been identified in drinking water (Wu et al., 2022; Yang and Zhang, 2016), most of which are halogenated DBPs including chlorinated DBPs (Cl-DBPs), brominated DBPs (Br-DBPs), and iodinated disinfection byproducts (I-DBPs). Therein, I-DBPs are more cytotoxic and genotoxic than Cl-DBPs and Br-DBPs (MacKeown et al., 2020; Richardson et al., 2007) and the formation of I-DBPs is primarily resulted from the disinfection of iodide-containing waters. The total iodine concentration of surface waters is mostly in range of 0.5–100 μg/L, which is lower than that of ground waters and sea waters (MacKeown et al., 2022). The iodine in waters can be originated from iodine-containing organic compound besides the inorganic iodine species (e.g., iodide (I^-) and iodate (IO_3^-)). Iodinated X-ray contrast media (ICM), widely used in the medical imaging of soft tissues, is considered as an important source of iodine in surface and ground waters (MacKeown et al., 2022). Particularly, iopamidol (IPM) is a representative of ICM. Although ICM is reported to be nontoxic, it could not be degraded by the biological process, which makes it accumulate easily in aquatic environment and be the organic iodine precursors of I-DBPs (Cao et al., 2021; Wang et al., 2019).

Advanced oxidation processes (AOPs) such as UV/hydrogen peroxide (H_2O_2), UV/chlorine (Cl_2), ozone/peroxymonosulfate (O_3/PMS), and Fe(II)/sulfite processes are the important methods for the degradation of ICM in water and wastewater treatment (Cha et al., 2022; Gao et al., 2022b; Mao et al., 2020; Zhao et al., 2019). Recently, the sulfite (refer to the equilibrium mixture of HSO_3^- and SO_3^{2-} in this study)-coupling permanganate (Mn(VII)/S(IV)) process has been proposed as a novel AOP that can oxidize various organic contaminants at extraordinarily high rates (for example, 60–150 sec^{-1}, pH_{ini} 5.0) (Sun et al., 2015). It is proved that multiple active oxidants including hydroxyl radical ($HO^{\cdot}$), sulfate radical ($SO_4^{\cdot-}$), and reactive manganese species (RMnS) are generated in the Mn(VII)/S(IV) process (Chen et al., 2020). Furthermore, the Mn(VII)/S(IV) system can be used as a pre-oxidation process to enhance the performance of subsequent coagulation due to the in-situ generation of MnO_2 during the Mn(VII)/S(IV) pre-oxidation (Chen et al., 2021; Zhu et al., 2020). Due to multiple active oxidants generated in this process, the mechanism for the degradation of ICM in the Mn(VII)/S(IV) pre-oxidation could be complicated. Moreover, the fate of iodine species during the degradation of ICM by the Mn(VII)/S(IV) process and the effect of the Mn(VII)/S(IV) pre-oxidation on the subsequent formation of I-DBPs during chlorination remain unknown.

Therefore, in this study, IPM was selected as the target compound and the objectives of this study are to (i) investigate the degradation kinetics of IPM in the Mn(VII)/S(IV) process, (ii) clarify the contribution of active oxidants to the degradation of IPM in the Mn(VII)/S(IV) process, (iii) determine the fate of iodine species during the degradation of IPM by the Mn(VII)/S(IV) process, and (iv) evaluate the subsequent formation and toxic risk of I-DBPs during chlorination.

1. Materials and methods

1.1. Chemicals and reagents

The complete list of reagents is provided in **Appendix A Text S1**. Colloidal MnO_2 stock solutions were prepared by mixing permanganate (Mn(VII)) and $Na_2S_2O_3$ stock solutions in stoichiometric ratio (Perez-Benito and Arias, 1992).

1.2. Experimental procedures

1.2.1. Pre-oxidation

The degradation of IPM in the Mn(VII)/S(IV) process was conducted at pH 7.0 and 8.0 in the presence of humic acid (HA). Borate (10 mmol/L) was used as a buffer for the experiments performed at pH 7.0 and 8.0. Solution pH was monitored by a Shanghai Leici pH meter.

Sulfite (HSO_3^-/SO_3^{2-}) could be dosed via one-time mode and multiple-times mode during the degradation of IPM in the Mn(VII)/S(IV) process. For the one-time mode, the working solutions containing IPM, sulfite, HA, and the substrate of interest were prepared and adjusted to the desired pH. Then, the desired concentration of Mn(VII) was added to initiate the reaction. For the multiple-times mode, the working solutions containing IPM, HA, and the substrate of interest were prepared and adjusted to the determined pH. Then, the desired concentration of Mn(VII) was dosed into the working solution, and sulfite was dosed immediately at a rate of 5.0 μmol/L per 10 sec. Periodically, a 5.0 mL sample was collected and immediately quenched using an excess sodium thiosulfate stock solution.

All experiments were performed at room temperature (25 ± 2°C). All samples were filtered by a suction filter device equipped with the mixed cellulose filter membrane (0.22 μm) before analysis.

1.2.2. Chlorination

The chlorination experiments were carried out in amber glass bottles capped with Teflon-faced septa. After pre-oxidation, the working solution was filtered by a suction filter device equipped with the mixed cellulose filter membrane (0.22 μm). Then, NaClO stock solution was dosed into the filtered solution. The chlorine dosages were determined by the concentration of the residual chlorine, which should be kept at the concentration of 1.0 ± 0.2 mg/L after 24 hr incubation at 25 ± 1°C in the dark. The concentration of the residual chlorine was detected with HACH method 8021 (detection range of 0.2–2.0 mg/L) using a HACH portable spectrophotometer (DR3900). Ascorbic acid was used to quench the residual chlorine for the subsequent DBPs detection.

1.2.3. Competitive oxidation kinetic experiments

Competitive oxidation kinetic experiments were performed to explore the relative contribution of $HO^{\cdot}$, $SO_4^{\cdot-}$, and RMnS to the degradation of IPM in the Mn(VII)/S(IV) process. The corresponding details are provided in **Appendix A Text S2** and **Figs. S1–S2**.

1.3. Analytical methods

1.3.1. UPLC analysis of target organic contaminants

The concentrations of organic contaminants residuals in samples were determined by an ultraperformance liquid chromatograph (UPLC, Waters ACQUITY UPLC H-Class) equipped with a UV detector. The compounds were separated by a BEH C18 column (2.1 × 100 mm, 1.7 μm; Waters Co.) in an isocratic mode of elution at 35 ± 1°C. The injection volume was 10 μL. The detailed analytical parameters are listed in **Appendix A Table S1**.

1.3.2. Measurement of DBPs

All DBPs were detected by a gas chromatograph (GC) (2010 plus, Shimadzu, Japan) equipped with an electron capture detector (ECD). The detailed analytical procedures and parameters are shown in **Appendix A Text S3** and **Table S2**. The relative standard deviations were 1.0%–10%.

1.3.3. Detection of inorganic ions

I^- and IO_3^- in samples were detected by an ion chromatograph (ICS-5000, Dionex, USA) equipped with a Dionex AS19 analytical column (2 × 250 mm) and an AG19 guard column (2 × 50 mm). The concentration of HOI was analyzed by the 2,6-dibromophenol capture method (Zhao et al., 2016).

1.3.4. Transformation products analysis

The transformation products of IPM were identified using a UPLC (Agilent 1290) coupled with a triple quadrupole MS system (UPLC-QqQ MS) and an electrospray ionization source (EIS, Agilent 6430). A BEH C18 column (100 mm × 2.1 mm, 1.7 μm; Waters, Milford, USA) with the controlled temperature of 45°C was applied to separate the transformation products. The injection volume was 20 μL, and a parent ion scanning mode (*m*/z 100–600) was used. The details of gradient elution are shown in **Appendix A Table S3**. The samples were extracted and desalinated by solid phase extraction (SPE, Thermo Fisher Scientific Co., Ltd.) with Poly-Sery HLB cartridge (150 mg, ANPEL, Shanghai, China) before the analysis of transformation products.

2. Results and discussion

2.1. The degradation kinetics of IPM in the Mn(VII)/S(IV) process

In this study, the influence of dosing modes of sulfite on the degradation of IPM in the Mn(VII)/S(IV) process was investigated under different sulfite concentrations at pH 7.0 and 8.0 (Fig. 1a). The dosing modes of sulfite had negligible influence on the degradation of IPM when the concentration of sulfite was 100 μmol/L. The degradation of IPM by multiple times dosing (80%) was much higher than that by one time dosing (37%) when the concentration of sulfite was 200 μmol/L. The difference in the removal of IPM between these two dosing modes of sulfite increased with increasing sulfite concentration. In the Mn(VII)/S(IV) process, sulfite was not only the precursor for the generation of active oxidants, but also consumed the generated active oxidants. For example, $SO_4^{\cdot-}$ could react with sulfite at high rates ($k_{SO_4^{\cdot-},\ HSO_3^-/SO_3^{2-}} = 2 \times 10^9$ L·mol^{-1}·sec^{-1}) (Huie and Neta, 1987). Therefore, multiple times dosing mode of sulfite can decrease the consumption of active oxidants by sulfite and increase the utilization of active oxidants in the Mn(VII)/S(IV) process. It should be noted that although Mn(VII) could be consumed up by 100 μmol/L sulfite, the continuous degradation of IPM could occur at 100–400 μmol/L sulfite, which could be due to the activation of sulfite by the in situ generated MnO_2 (**Appendix A Fig. S3**) (Chen et al., 2020; Sun et al., 2015; Sun et al., 2019). In addition, the degradation of IPM can be almost negligible in the solutions containing Mn(VII), Mn(IV), or sulfite alone (**Appendix A Fig. S4**). Therefore, the multiple times dosing mode of sulfite was employed in the subsequent experiments about the Mn(VII)/S(IV) process.

It is documented that HA, as a substitute of NOM, widely exists in the aquatic environment, and is considered as the important precursor of DBPs (Yang et al., 2022b). In this study, the influence of HA concentrations on the degradation of IPM in the Mn(VII)/S(IV) process was investigated at pH 7.0 and pH 8.0 (Fig. 1b and c). The degradation of IPM was inhibited slightly in the presence of 0.5–2.0 mg C/L HA while the inhibition became obvious in the presence of 5.0 mg C/L HA. Regardless of the HA concentration, the removal of IPM increased with increasing sulfite concentration. The removal of IPM were 89% and 94% at pH 7.0 and 8.0, respectively, when the concentration of sulfite was 600 μmol/L in the presence of 2.0 mg C/L HA. In sum, the fate of iodine species during the degradation of IPM in the Mn(VII)/S(IV) process, and the subsequent formation of DBPs during chlorination were subsequently investigated in the presence of 2.0 mg C/L HA. Furthermore, the degradation of IPM in the Mn(VII)/S(IV) process was not affected by the solution pH, which might be ascribed to the nature of active oxidants generated in the Mn(VII)/S(IV) process.

2.2. The role of active oxidants in the Mn(VII)/S(IV) process

It is reported that multiple active oxidants ($HO^{\cdot}$, $SO_4^{\cdot-}$, and RMnS) are generated in the Mn(VII)/S(IV) process. In order to comprehensively illustrate the mechanism of IPM degradation in this process, it is necessary to identify the role of active oxidants in the degradation of IPM in the Mn(VII)/S(IV) process. Methanol (MeOH) and tert-butanol (TBA) were widely used as scavengers due to their different reactivity toward $HO^{\cdot}$ and $SO_4^{\cdot-}$ ($k_{HO^{\cdot},\ MeOH} = 9.7 \times 10^8$ L·mol^{-1}·sec^{-1}, $k_{HO^{\cdot},\ TBA} = 6.0 \times 10^8$ L·mol^{-1}·sec^{-1}, $k_{SO_4^{\cdot-},\ MeOH} = 2.5 \times 10^7$ L·mol^{-1}·sec^{-1}, and $k_{SO_4^{\cdot-},\ TBA} = 9.1 \times 10^5$ L·mol^{-1}·sec^{-1}) (Buxton et al., 1988; Neta et al., 1988). Halogen ions (Cl^-, Br^-) could react with radicals ($HO^{\cdot}$ and $SO_4^{\cdot-}$)

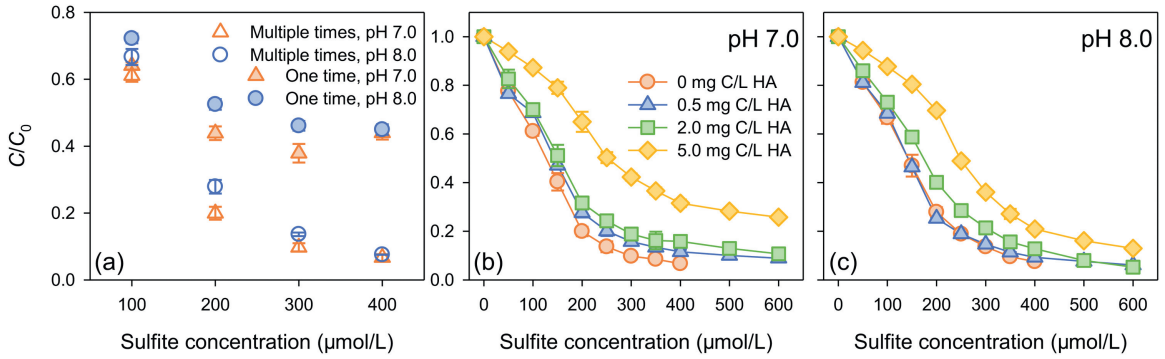

Fig. 1 – (a) Influence of sulfite dosing mode on the degradation of IPM in the Mn(VII)/S(IV) process under different sulfite concentrations in the absence of HA. (b–c) Degradation kinetics of IPM by multiple times dosing in the Mn(VII)/S(IV) process in the presence of HA at pH 7.0 and 8.0. Reaction conditions: $[Mn(VII)]_0$ = 50 μmol/L, $[IPM]_0$ = 3.0 μmol/L. In the one-time dosing mode, the reaction time is 5.0 sec. In the multiple-times dosing mode, sulfite dosing rate is 5.0 μmol/L per 10 sec.

at higher rates ($k_{HO^{\cdot},\,Cl^-}$ = 4.3 × 10^9 L·mol^{-1}·sec^{-1}, $k_{HO^{\cdot},\,Br^-}$ = 1.1 × 10^{10} L·mol^{-1}·sec^{-1}, $k_{SO_4^{\cdot-},\,Cl^-}$ = 3.1 × 10^8 L·mol^{-1}·sec^{-1}, and $k_{SO_4^{\cdot-},\,Br^-}$ = 3.5 × 10^9 L·mol^{-1}·sec^{-1}) (Buxton et al., 1988; Neta et al., 1988). Nevertheless, RMnS has negligible reactivity toward these alcohols (MeOH and TBA) and halogen ions (Cl^- and Br^-) (Chen et al., 2020). In the **Appendix A Fig. S5a**, both MeOH and TBA could significantly inhibit the degradation of IPM in the Mn(VII)/S(IV) process. The degradation of IPM decreased from 92% to 30% at pH 8.0 in the presence of 10 mmol/L MeOH when the concentration of sulfite was 400 μmol/L. The degradation of IPM was almost inhibited in the presence of 100 mmol/L MeOH. Nevertheless, the degradation of IPM just decreased to 70% in the presence of 10 mmol/L TBA and 31% in the presence of 100 mmol/L TBA. In **Appendix A Fig. S5b**, the degradation of IPM decreased from 95% to 60% and 30% at pH 8.0 in the presence of 1.0 mmol/L and 10 mmol/L Cl^-, respectively, when the concentration of sulfite was 400 μmol/L. Furthermore, the similar inhibition on the degradation of IPM was also observed in the presence of 10 μmol/L and 100 μmol/L Br^-. These results indicated that free radicals play an important role in the degradation of IPM in the Mn(VII)/S(IV) process and $SO_4^{\cdot-}$ may contribute more to the degradation of IPM than $HO^{\cdot}$. However, recent studies proposed that the quenching experimental results in AOPs might come to a wrong conclusion and then made us misunderstand the role of active oxidants (Gao et al., 2022a; Guo et al., 2022; Wang et al., 2022a). Therefore, more solid evidence is needed to determine the contributions of these active oxidants to the degradation of IPM in the Mn(VII)/S(IV) process.

Competitive oxidation kinetic experiments were conducted to distinguish the contributions of $SO_4^{\cdot-}$, $HO^{\cdot}$, and RMnS to the degradation of IPM in the Mn(VII)/S(IV) process (Figs. 2 and Appendix A Fig. **S1**). The contribution of $SO_4^{\cdot-}$ to the degradation of IPM in the Mn(VII)/S(IV) process at pH 8.0 was almost 100% whereas the contributions of $HO^{\cdot}$ and RMnS were negligible. The contributions of active oxidants to the degradation of IPM depend on the second-order rate constants of active oxidants with IPM and the steady-state concentration of active oxidants. The second-order rate constants of IPM with $HO^{\cdot}$ was lower than that with $SO_4^{\cdot-}$ ($k_{HO^{\cdot},\,IPM}$ = 1.8 × 10^9 L·mol^{-1}·sec^{-1} and $k_{SO_4^{\cdot-},\,IPM}$ = 2.7 × 10^9 L·mol^{-1}·sec^{-1}), and the calculated second-order rate constants of IPM with $HO^{\cdot}$ and $SO_4^{\cdot-}$ in this study were consistent with the reported values in the literature (Cao et al., 2021; Jeong et al., 2010). Meanwhile, the steady-state concentration of $HO^{\cdot}$ was also lower than that of $SO_4^{\cdot-}$ since $HO^{\cdot}$ was mainly generated from the reaction of $SO_4^{\cdot-}$ with H_2O/OH^- in the Mn(VII)/S(IV) process ($k_{SO_4^{\cdot-},\,OH^-}$ = (6.5 ± 1.0) × 10^7 L·mol^{-1}·sec^{-1}, $k_{SO_4^{\cdot-},\,H_2O}$ = (6.6 ± 0.4) × 10^2 sec^{-1}) (Hayon et al., 1972; Herrmann et al., 1995), which was also supported by the experimental results shown in the **Appendix A Fig. S1**. Therefore, the contribution of $HO^{\cdot}$ to IPM degradation was tiny in the Mn(VII)/S(IV) process. Furthermore, the negligible contribution of RMnS might be ascribed to the low steady-state concentration of RMnS and the reactivity of RMnS toward IPM (Kirschenbaum and Meyerstein, 1981; Lee and Chen, 1989; Lee et al., 2020; Rush and Bielski, 1995; Shao et al., 2022a; Wang et al., 2022b). In sum, $SO_4^{\cdot-}$ was verified to be mainly responsible for the degradation of IPM in the Mn(VII)/S(IV) process.

2.3. *The fate of iodine species during the degradation of IPM in the Mn(VII)/S(IV) process*

The evolution of iodine species during the degradation of IPM with the Mn(VII)/S(IV) pre-oxidation is related to the subsequent formation of I-DBPs during chlorination. Therefore, it is necessary to investigate the fate of iodine species during the degradation of IPM in the Mn(VII)/S(IV) process. As shown in Fig. 3, the released inorganic iodine species during the degradation of IPM in the Mn(VII)/S(IV) process were I^- and IO_3^- and the concentration of I^- and IO_3^- increased with increasing sulfite concentration at pH 7.0 and 8.0. The concentration of inorganic iodine species would be 8.0 μmol/L with 600 μmol/L sulfite if the iodine species in the degraded IPM (89%) was totally released at pH 7.0 in the Mn(VII)/S(IV) process. Nevertheless, the concentrations of I^- and IO_3^- were 4.1 μmol/L and 1.6 μmol/L, respectively, with 600 μmol/L sulfite in the Mn(VII)/S(IV) process at pH 7.0. The total concentration of inorganic iodine (5.7 μmol/L) was lower than the theoretical value (8 μmol/L) at pH 7.0, indicating that iodine-containing organic

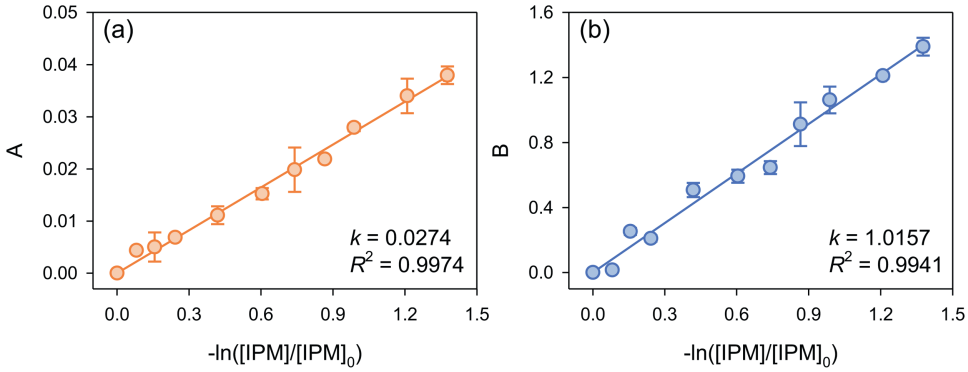

Fig. 2 – Plots of (a) A versus $-\ln([IPM]/[IPM]_0)$ and (b) B versus $-\ln([IPM]/[IPM]_0)$ in the Mn(VII)/S(IV) process ($-k_{IPM,\ HO\cdot}\ln([p\text{-}NBA]/[p\text{-}NBA]_0/k_{p-NBA,\ HO\cdot}$ denoted as A, and $-k_{IPM,\ SO_4^{\cdot-}}(\ln([p\text{-}CBA]/[p\text{-}CBA]_0 - k_{p-CBA,\ HO\cdot}\ln([p\text{-}NBA]/[p\text{-}NBA]_0/k_{p-NBA,\ HO\cdot})/k_{p-CBA,\ SO_4^{\cdot-}})$ denoted as B). Reaction conditions: $[Mn(VII)]_0 = 50$ μmol/L, $[IPM]_0 = [p\text{-}CBA]_0 = [p\text{-}NBA]_0 = 5.0$ μmol/L, pH = 8.0. The sulfite dosing rate is 5.0 μmol/L per 10 sec.

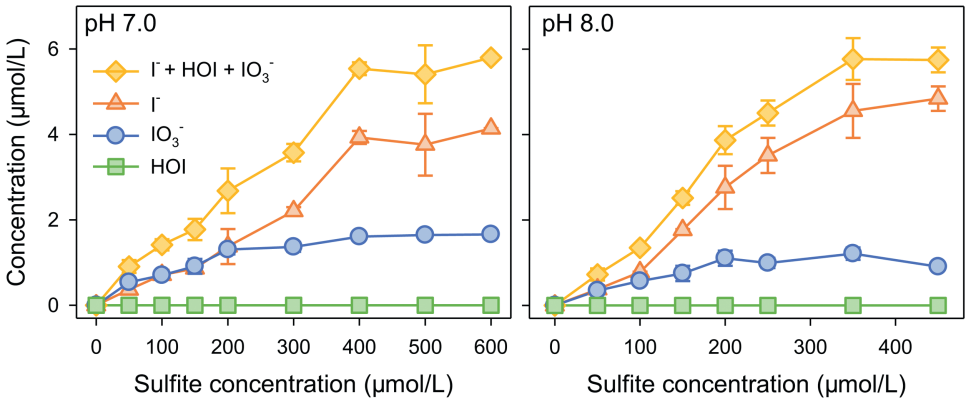

Fig. 3 – Evolution of I^-, HOI, and IO_3^- during the degradation of IPM in the Mn(VII)/S(IV) process. Reaction conditions: $[Mn(VII)]_0 = 50$ μmol/L, $[IPM]_0 = 3.0$ μmol/L, $[HA]_0 = 2.0$ mg C/L. The sulfite dosing rate is 5.0 μmol/L per 10 sec.

products were also produced during the degradation of IPM in the Mn(VII)/S(IV) process at pH 7.0. Moreover, the concentrations of I^- and IO_3^- were 4.8 μmol/L and 0.9 μmol/L, respectively, and the sum amount of I^- and IO_3^- was lower than the theoretical value (7.65 μmol/L, 85% of IPM was degraded) with 450 μmol/L sulfite in the Mn(VII)/S(IV) process at pH 8.0. I^- was firstly released during the degradation of IPM in the Mn(VII)/S(IV) process. Since the steady-state concentration of $HO^\cdot$ was lower than that of $SO_4^{\cdot-}$ in the Mn(VII)/S(IV) process, the released I^- could be mainly further oxidized by $SO_4^{\cdot-}$. I^- could react with $SO_4^{\cdot-}$ (Eqs. (1)-(5)) to generate $I^\cdot$, and HOI would be generated from the further reactions involving $I^\cdot$ and I^- (MacKeown et al., 2022; Shao et al., 2022b; Wang et al., 2017). The formed HOI could be further oxidized by $SO_4^{\cdot-}$ to produce IO_3^-. Moreover, HOI could also be reduced back to I^- by sulfite. In addition, RMnS showed low reactivity toward these inorganic iodine species. Therefore, no HOI was detected during the degradation of IPM and the formation of IO_3^- was not significant in the Mn(VII)/S(IV) process. In sum, the released inorganic iodine species during the degradation of IPM in the Mn(VII)/S(IV) process were I^- and IO_3^-, and the concentration of I^- was higher than that of IO_3^-.

$$SO_4^{\cdot-} + I^- \rightarrow I^\cdot + SO_4^{2-} \quad (1)$$

$$I^\cdot + I^- \rightarrow I_2^{\cdot-} \quad (2)$$

$$I_2^{\cdot-} + I^\cdot \rightarrow I_2 + I^- \quad (3)$$

$$I_2^{\cdot-} + I_2^{\cdot-} \rightarrow I_2 + I^- \quad (4)$$

$$I_2 + H_2O \rightarrow HOI + I^- + H^+ \quad (5)$$

2.4. *The subsequent formation and toxicity evaluation of I-DBPs during chlorination*

The subsequent formation of DBPs during chlorination with the Mn(VII)/S(IV) pre-oxidation was investigated and the results are shown in Fig. 4. Five Cl-DBPs, i.e., chloroform (TCM), dichloroacetonitrile (DCAN), 1,1,1-trichloro-2-propanone (1,1,1-TCP), dichloroacetic acid (DCAA), and trichloroacetic

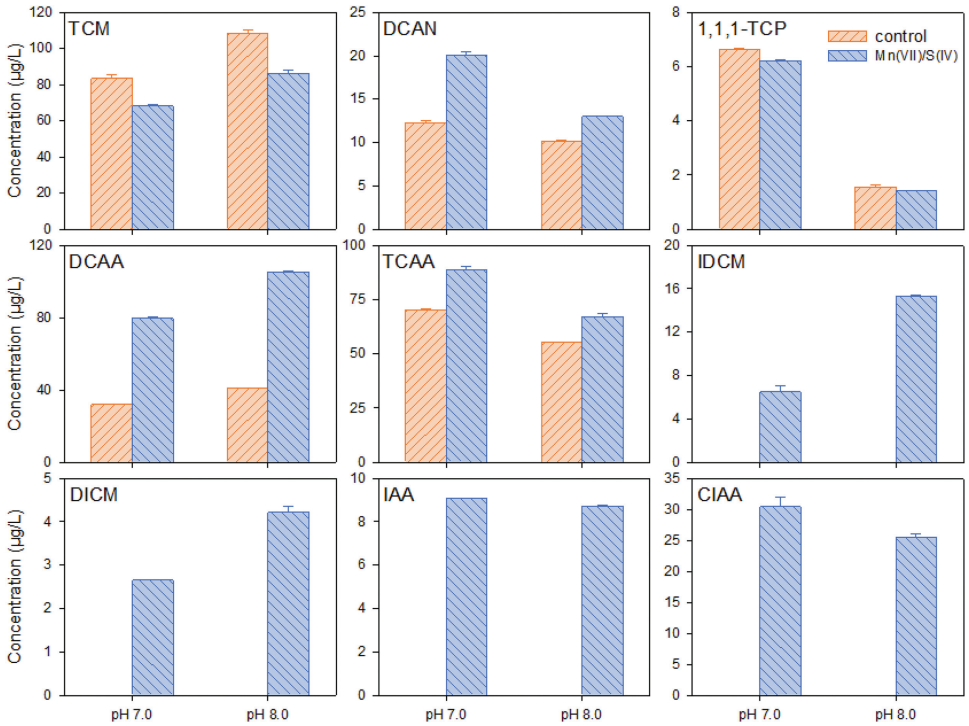

Fig. 4 – DBPs generation during chlorination after pre-oxidation by the Mn(VII)/S(IV) process in synthetic water. Reaction conditions: $[Mn(VII)]_0$ = 50 μmol/L, $[IPM]_0$ = 3.0 μmol/L, $[HA]_0$ = 2.0 mg C/L. The sulfite dosing rate is 5.0 μmol/L per 10 sec. The chlorination time was 24 hr.

acid (TCAA), and four I-DBPs, i.e., iododichloromethane (IDCM), diiodochloromethane (DICM), iodoacetic acid (IAA), and iodochloroacetic acid (CIAA), were detected during chlorination. The concentration of TCM and 1,1,1-TCP in the chlorination alone was higher than that with the Mn(VII)/S(IV) pre-oxidation whereas the amount of DCAN, DCAA, and TCAA generated during chlorination alone was lower than that with the Mn(VII)/S(IV) pre-oxidation at pH 7.0 and 8.0. These results indicated that the influence of the Mn(VII)/S(IV) pre-oxidation on the subsequent formation of Cl-DBPs was related to the category of Cl-DBPs. Four I-DBPs (IDCM, DICM, IAA, and CIAA) were not formed during chlorination without pre-oxidation but generated during chlorination with the Mn(VII)/S(IV) pre-oxidation. This result showed that the inorganic and organic products generated from the pre-oxidation of IPM reacted more readily with chorine than IPM to form I-DBPs. The formation of I-DBPs during chlorination with the Mn(VII)/S(IV) pre-oxidation was mainly resulted from the reaction of chlorine with the transformation products of IPM (**Appendix A Table S4**) and the inorganic iodine species released during the degradation of IPM in the Mn(VII)/S(IV) process (Fig. 3) (Dong et al., 2019; Li et al., 2020; MacKeown et al., 2022). The transformation products of IPM in the Mn(VII)/S(IV) process might react with chlorine to form I-DBPs during chlorination. During chlorination, the released I^- after the Mn(VII)/S(IV) pre-oxidation would be rapidly oxidized by chlorine to form HOI, but the transformation of HOI to IO_3^- was slow. Therefore, HOI was accumulated and further reacted with HA to generate I-DBPs during chlorination (MacKeown et al., 2022). Moreover, the formation of IDCM and DICM with pre-oxidation was more sensitive to the solution pH than that of IAA and CIAA. Since the toxic risk derived from each DBPs was different, it was hard to assess how the pre-oxidation of IPM by the Mn(VII)/S(IV) process has effects on the DBPs toxicity only via determining the concentration of each DBP during chlorination. Therefore, it was necessary to evaluate the toxicity of these DBPs.

Integrated toxic risk value (ITRV) was applied to further evaluate the influence of the Mn(VII)/S(IV) pre-oxidation on the toxicity of DBPs (**Appendix A Text S4, Table S5**, and Fig. 5). In Fig. 5, ITRVs of DBPs generated during chlorination with the Mn(VII)/S(IV) pre-oxidation were 34–36 times higher than that without pre-oxidation, which was due to the generation of I-DBPs with the Mn(VII)/S(IV) pre-oxidation. These results indicated that the pre-oxidation of IPM by the Mn(VII)/S(IV) process was not conducive to control the toxic risk caused by the subsequent formation of I-DBPs. Furthermore, ITRVs of DBPs generated during chlorination with pre-oxidation were mainly donated by IAA (**Appendix A Table S5**). Overall, the influence of the IPM pre-oxidation by the Mn(VII)/S(IV) process on the toxic risk of DBPs should be noted.

3. Conclusions

In the present study, we investigated the degradation of IPM and the evolution of iodine species in the Mn(VII)/S(IV) process, and the subsequent formation of I-DBPs during chlorination at pH 7.0 and 8.0. The removal of IPM in the Mn(VII)/S(IV) process could be more than 89% in the presence of 2.0 mg/L

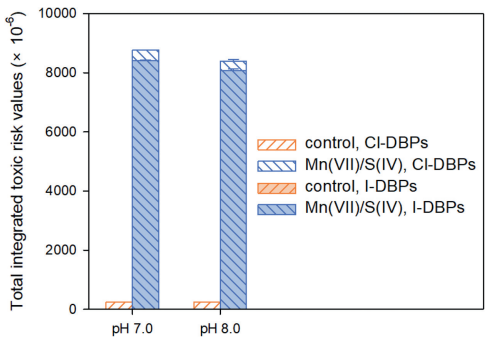

Fig. 5 – The calculated integrated toxic risk values of DBPs generated during chlorination after pre-oxidation by the Mn(VII)/S(IV) process in synthetic water. Reaction conditions: $[Mn(VII)]_0$ = 50 μmol/L, $[IPM]_0$ = 3.0 μmol/L, $[HA]_0$ = 2.0 mg C/L. The sulfite dosing rate is 5.0 μmol/L per 10 sec. The chlorination time was 24 hr.

HA at pH 7.0 and 8.0 when the concentration of sulfite was 600 μmol/L. $SO_4^{\cdot-}$ mainly contributed to the degradation of IPM in the Mn(VII)/S(IV) process whereas the contributions of $HO^{\cdot}$ and RMnS were negligible. The released inorganic iodine species during the degradation of IPM in the Mn(VII)/S(IV) process were I^- and IO_3^-, and the concentration of I^- was higher than that of IO_3^-. The results about Cl-DBPs indicated that the Mn(VII)/S(IV) pre-oxidation had different effects on the subsequent formation of different Cl-DBPs during chlorination. Nevertheless, the subsequent formation of I-DBPs during the chlorination with the Mn(VII)/S(IV) pre-oxidation was higher at pH 7.0 and 8.0 than that without pre-oxidation, and the ITRVs of DBPs generated during chlorination with the Mn(VII)/S(IV) pre-oxidation at pH 7.0 and 8.0 were much higher than that without pre-oxidation. Although the Mn(VII)/S(IV) process can degrade IPM effectively, the total toxicity of DBPs with the Mn(VII)/S(IV) pre-oxidation increased due to the subsequent formation of I-DBPs. The similar phenomenon was observed in the degradation of IPM by other pre-oxidation process such as the UV/Cl_2 process and the UV/H_2O_2 process (Dong et al., 2018; Sengar and Vijayanandan, 2021; Tian et al., 2020; Yang et al., 2022a; Zhao et al., 2019). Therefore, it should be noted that the pre-oxidation might be an inappropriate choice for the iodide-containing water treatment. More attention should be paid to the toxicity of DBPs generated from the iodide-containing water treatment.

Declaration of Competing Interest

The authors declare that they have no known competing financial interests or personal relationships that could have appeared to influence the work reported in this paper.

Acknowledgments

This work was supported by the National Natural Science Foundation of China (Nos. 22206050, 22025601, 21976133 and 52270047), the National Key Research and Development Program of China (No. 2019YFC1805202), and the State Key Laboratory of Pollution Control and Resource Reuse Foundation (No. PCRRK20014).

Appendix A Supplementary data

Supplementary material associated with this article can be found, in the online version, at doi:10.1016/j.jes.2022.11.020.

REFERENCES

Buxton, G.V., Greenstock, C.L., Helman, W.P., Ross, A., 1988. Critical review of rate constants for reactions of hydrated electrons, hydrogen atoms and hydroxyl radicals $HO^{\cdot}/O^{-}$ in aqueous solution. J. Phys. Chem. Ref. Data 17, 513–886.

Cao, Y., Qiu, W., Li, J., Zhao, Y., Jiang, J., Pang, S., 2021. Sulfite enhanced transformation of iopamidol by UV photolysis in the presence of oxygen: role of oxysulfur radicals. Water Res. 189, 116625.

Cha, Y., Kim, T.K., Lee, J., Kim, T., Hong, A.J., Zoh, K.D., 2022. Degradation of iopromide during the UV-LED/chlorine reaction: effect of wavelength, radical contribution, transformation products, and toxicity. J. Hazard. Mater. 437, 129371.

Chen, J., Ling, J., Sun, B., Wang, J., Zhou, B., Guan, X., et al, ., 2021. Trace organic contaminants abatement by permanganate/bisulfite pretreatment coupled with conventional water treatment processes: lab- and pilot-scale tests. J. Hazard. Mater. 401, 123380.

Chen, J., Rao, D., Dong, H., Sun, B., Shao, B., Cao, G., et al, ., 2020. The role of active manganese species and free radicals in permanganate/bisulfite process. J. Hazard. Mater. 388, 121735.

Dong, H., Qiang, Z., Liu, S., Li, J., Yu, J., Qu, J., 2018. Oxidation of iopamidol with ferrate (Fe(VI)): kinetics and formation of toxic iodinated disinfection by-products. Water Res. 130, 200–207.

Dong, H., Qiang, Z., Richardson, S.D., 2019. Formation of iodinated disinfection byproducts (I-DBPs) in drinking water: emerging concerns and current issues. Accounts Chem. Res. 52, 896–905.

Gao, L., Guo, Y., Zhan, J., Yu, G., Wang, Y., 2022a. Assessment of the validity of the quenching method for evaluating the role of reactive species in pollutant abatement during the persulfate-based process. Water Res. 221, 118730.

Gao, Y., Fan, W., Zhang, Z., Zhou, Y., Zeng, Z., Yan, K., et al., 2022b. Transformation mechanisms of iopamidol by iron/sulfite systems: involvement of multiple reactive species and efficiency in real water. J. Hazard. Mater. 426, 128114.

Guo, Y., Long, J., Huang, J., Yu, G., Wang, Y., 2022. Can the commonly used quenching method really evaluate the role of reactive oxygen species in pollutant abatement during catalytic ozonation? Water Res. 215, 118275.

Hayon, E., Treinin, A., Wilf, J., 1972. Electronic spectra, photochemistry, and autoxidation mechanism of the sulfite-bisulfite-pyrosulfite systems. SO_2^-, SO_3^-, SO_4^-, and SO_5^- radicals. J. Am. Chem. Soc. 94, 47–57.

Herrmann, H., Reese, A., Zellner, R., 1995. Time-resolved UV/VIS diode array absorption spectroscopy of SO_x^- ($_x$=3, 4, 5) radical anions in aqueous solution. J. Mol. Struct. 348, 183–186.

Huie, R.E., Neta, P., 1987. Rate constants for some oxidations of S(IV) by radicals in aqueous solutions. Atmos. Environ. 21, 1743–1747.

Jeong, J., Jung, J., Cooper, W.J., Song, W., 2010. Degradation mechanisms and kinetic studies for the treatment of X-ray

contrast media compounds by advanced oxidation/reduction processes. Water Res. 44, 4391–4398.
Kirschenbaum, L.J., Meyerstein, D., 1981. A pulse radiolysis study of the MnO_4^{2-} ion. The stability of Mn(V) in 0.1 M NaOH. Inorg. Chim. Acta 53, L99–L100.
Lee, D.G., Chen, T., 1989. Oxidation of hydrocarbons. 18. Mechanism of the reaction between permanganate and carbon-carbon double bonds. J. Am. Chem. Soc. 111, 7534–7538.
Lee, J., von Gunten, U., Kim, J.H., 2020. Persulfate-based advanced oxidation: critical assessment of opportunities and roadblocks. Environ. Sci. Technol. 54, 3064–3081.
Li, J., Jiang, J., Pang, S.Y., Cao, Y., Zhou, Y., Guan, C., 2020. Oxidation of iodide and hypoiodous acid by non-chlorinated water treatment oxidants and formation of iodinated organic compounds: a review. Chem. Eng. J. 386, 123822.
MacKeown, H., Adusei Gyamfi, J., Schoutteten, K.V.K.M., Dumoulin, D., Verdickt, L., Ouddane, B., et al, ., 2020. Formation and removal of disinfection by-products in a full scale drinking water treatment plant. Sci. Total Environ. 704, 135280.
MacKeown, H., von Gunten, U., Criquet, J., 2022. Iodide sources in the aquatic environment and its fate during oxidative water treatment – a critical review. Water Res. 217, 118417.
Mao, Y., Dong, H., Liu, S., Zhang, L., Qiang, Z., 2020. Accelerated oxidation of iopamidol by ozone/peroxymonosulfate (O_3/PMS) process: kinetics, mechanism, and simultaneous reduction of iodinated disinfection by-product formation potential. Water Res. 173, 115615.
McGuire, M.J., 2006. Eight revolutions in the history of US drinking water disinfection. J. AWWA 98, 123–149.
Neta, P., Huie, R.E., Ross, A.B., 1988. Rate constants for reactions of inorganic radicals in aqueous solution. J. Phys. Chem. Ref. Data 17, 1027–1284.
Perez-Benito, J.F., Arias, C., 1992. Occurrence of colloidal manganese dioxide in permanganate reactions. J. Colloid Interface Sci. 152, 70–84.
Richardson, S.D., Plewa, M.J., Wagner, E.D., Schoeny, R., DeMarini, D.M., 2007. Occurrence, genotoxicity, and carcinogenicity of regulated and emerging disinfection by-products in drinking water: a review and roadmap for research. Mutat. Res.-Rev. Mutat. Res. 636, 178–242.
Rush, J.D., Bielski, B.H.J., 1995. Studies of manganate(V), -(VI), and -(VII) tetraoxyanions by pulse radiolysis. Optical spectra of protonated forms. Inorg. Chem. 34, 5832–5838.
Sengar, A., Vijayanandan, A., 2021. Comprehensive review on iodinated X-ray contrast media: complete fate, occurrence, and formation of disinfection byproducts. Sci. Total Environ. 769, 144846.
Shao, B., Dong, H., Zhou, G., Ma, J., Sharma, V.K., Guan, X., 2022a. Degradation of organic contaminants by reactive iron/manganese species: progress and challenges. Water Res. 221, 118765.
Shao, B., Zhu, Y., Chen, J., Lin, Y., Guan, X., 2022b. Fate and transformation of iodine species during Mn(VII)/sulfite treatment in iodide-containing water. Water Environ. Res. 94, e10788.
Sun, B., Guan, X., Fang, J., Tratnyek, P.G., 2015. Activation of manganese oxidants with bisulfite for enhanced oxidation of organic contaminants: the involvement of Mn(III). Environ. Sci. Technol. 49, 12414–12421.
Sun, B., Xiao, Z., Dong, H., Ma, S., Wei, G., Cao, T., et al, ., 2019. Bisulfite triggers fast oxidation of organic pollutants by colloidal MnO_2. J. Hazard. Mater. 363, 412–420.
Tian, F.X., Ye, W.K., Xu, B., Hu, X.J., Ma, S.X., Lai, F., et al, ., 2020. Comparison of UV-induced AOPs (UV/Cl_2, UV/NH_2Cl, UV/ClO_2 and UV/H_2O_2) in the degradation of iopamidol: kinetics, energy requirements and DBPs-related toxicity in sequential disinfection processes. Chem. Eng. J. 398, 125570.
Wang, L., Kong, D., Ji, Y., Lu, J., Yin, X., Zhou, Q., 2017. Transformation of iodide and formation of iodinated by-products in heat activated persulfate oxidation process. Chemosphere 181, 400–408.
Wang, L., Li, B., Dionysiou, D.D., Chen, B., Yang, J., Li, J., 2022a. Overlooked formation of H_2O_2 during the hydroxyl radical-scavenging rrocess when using alcohols as scavengers. Environ. Sci. Technol. 56, 3386–3396.
Wang, X., Wang, Z., Tang, Y., Xiao, D., Zhang, D., Huang, Y., et al, ., 2019. Oxidative degradation of iodinated X-ray contrast media (iomeprol and iohexol) with sulfate radical: an experimental and theoretical study. Chem. Eng. J. 368, 999–1012.
Wang, Z., Qiu, W., Pang, S.Y., Guo, Q., Guan, C., Jiang, J., 2022b. Aqueous iron(IV)–oxo complex: an emerging powerful reactive oxidant formed by iron(II)-based advanced oxidation processes for oxidative water treatment. Environ. Sci. Technol. 56, 1492–1509.
Wu, Y., Wei, W., Luo, J., Pan, Y., Yang, M., Hua, M., et al., 2022. Comparative toxicity analyses from different endpoints: are new cyclic disinfection byproducts (DBPs) more toxic than common aliphatic DBPs? Environ. Sci. Technol. 56, 194–207.
Yang, M., Zhang, X., 2016. Current trends in the analysis and identification of emerging disinfection byproducts. Trends Environ. Anal. Chem. 10, 24–34.
Yang, T., Wu, S., Mai, J., Chen, L., Huang, C., Zeng, G., et al., 2022a. Activation of ferrate(VI) by sulfite for effectively degrading iodinated contrast media and synchronously controlling I-DBPs formation. Chem. Eng. J. 442, 136011.
Yang, X., Rosario-Ortiz, F.L., Lei, Y., Pan, Y., Lei, X., Westerhoff, P., 2022b. Multiple roles of dissolved organic matter in advanced oxidation processes. Environ. Sci. Technol. 56, 11111–11131.
Zhao, X., Jiang, J., Pang, S., Guan, C., Li, J., Wang, Z., et al, ., 2019. Degradation of iopamidol by three UV-based oxidation processes: kinetics, pathways, and formation of iodinated disinfection byproducts. Chemosphere 221, 270–277.
Zhao, X., Salhi, E., Liu, H., Ma, J., von Gunten, U., 2016. Kinetic and mechanistic aspects of the reactions of iodide and hypoiodous acid with permanganate: oxidation and disproportionation. Environ. Sci. Technol. 50, 4358–4365.
Zhu, Y., Ling, J., Li, L., Guan, X., 2020. The effectiveness of bisulfite-activated permanganate technology to enhance the coagulation efficiency of *Microcystis aeruginosa*. Chin. Chem. Lett. 31, 1545–1549.